

Supporting Information

Functionalization of transparent conductive oxide electrode for TiO₂-free perovskite solar cell

P. Topolovsek,^{a, c} F. Lamberti,^{a*} T. Gatti,^b A. Cito,^a J. M. Ball,^a E. Menna,^b C. Gadermaier^{c, d} and A. Petrozza^{a*}

^a Center for Nanoscience and Technology, Istituto Italiano di Tecnologia, Via Pascoli 70/3, 20133 Milano, Italy

^b Department of Chemical Sciences, University of Padova, Via Marzolo 1, 35131 Padova, Italy

^c Jozef Stefan International Postgraduate School, Jamova 39, 1000 Ljubljana, Slovenia

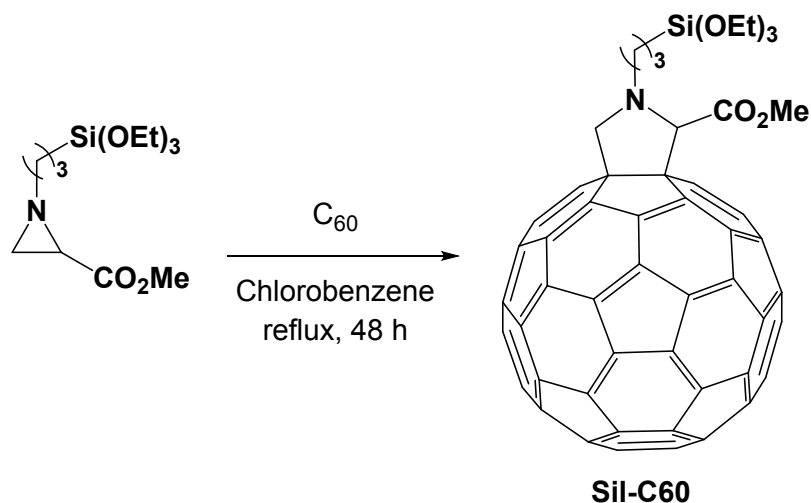
^d Jozef Stefan Institute, Jamova 39, 1000 Ljubljana, Slovenia

*Corresponding author(s): cescofanti@gmail.com; Annamaria.Petrozza@iit.it

Supporting Methods

Sil-C60 preparation. All reagents and solvents were purchased from Sigma Aldrich and used as received. C₆₀ was purchased from BuckyUSA (98+%).

The synthesis of **Sil-C60** molecule has been described previously^[1] but is here reported again with slight modifications for the sake of clarity (see Scheme S1). *N*-[3-(triethoxysilyl)propyl]-2-carbomethoxyaziridine (**1**) was also prepared following the procedure reported in reference [1].



Scheme S1. Synthesis of *N*-[3-(Triethoxysilyl)propyl]-2-carbomethoxy-3,4-fulleropyrrolidine (**Sil-C60**).

***N*-[3-(Triethoxysilyl)propyl]-2-carbomethoxy-3,4-fulleropyrrolidine (Sil-C60).** C₆₀ (200 mg, 0.28 mmol) was added to degassed chlorobenzene (200 ml) under a nitrogen atmosphere. After stirring for 10 min, *N*-[3-(triethoxysilyl)propyl]-2-carbomethoxyaziridine (340 mg, 1.13 mmol) was

added and the resulting mixture was heated up to 130 °C for 48 h. After cooling down to room temperature, the solvent was evaporated and the residue was purified through column chromatography on silica gel, eluting initially with toluene to eliminate unreacted C₆₀ and then with toluene:ethyl acetate (8:2) to isolate the product. The combined fractions containing the product were concentrated to 5 ml and acetonitrile (20 ml) was added, inducing the precipitation of a brown solid. The dispersion was centrifuged (1500 rpm, 20 min) and the supernatant was removed. Fresh acetonitrile (20 ml) was added and, after sonication, the same centrifugation procedure was repeated. The brown solid at the bottom of the centrifugation vessel was dried in vacuo, resulting in 116 mg of pure **Sil-C60** (40%). ¹H NMR (300 MHz, CDCl₃) δ (ppm): 5.16 (s, 1H), 5.12 (d, 1H, *J* = 9 Hz), 4.38 (d, 1H, *J* = 9 Hz), 3.91 (m, 9H), 3.37 (m, 1H), 3.02 (m, 1H), 2.09 (m, 2H), 1.30 (t, 9H, *J* = 6 Hz), 0.88 (m, 2H). ¹³C NMR (CDCl₃, 75 MHz) δ (ppm): 170.42, 154.85, 154.74, 153.72, 151.16, 146.35, 146.31, 146.14, 146.12, 145.86, 145.83, 145.71, 145.5, 145.39, 145.37, 145.33, 142.75, 142.73, 142.69, 142.20, 142.17, 141.89, 77.66, 72.77, 69.59, 65.21, 58.59, 55.31, 52.19, 21.86, 18.55, 8.29. MALDI-MS (C₇₃H₂₇NO₅Si, MW = 1025) *m/z* 1025 [M]⁺, 965 [M-CO₂CH₃-H]⁺.

Supporting Results

Sample	R _s (Ohm)	R _{po} (Ohm)	C _c (nF)	R _{ct} (kOhm)	Q _{dl} (uMho)
Sil-C60 SAM	137 (1%)	733 (9%)	649 (3%)	90.9 (1.5%)	1.46 (4%) / N=0.876 (0.90%)
Sil-C60 SAM after DMF	132 (2%)	383 (17%)	675 (5%)	80.0 (2.4%)	2.62 (5%) / N=0.829 (1%)

Table S1. Summary of fitted data for Sil-C60 SAM sample using equivalent circuit model in Figure 1b of the main manuscript. CPEs are used instead of ideal capacitances for increasing the quality of the fitting ($\chi^2 < 0.03$)

R _s (Ohm)	R _{ct} ^{FTO} (kOhm)	Q _{dl} (uMho)	Q _w (mMho)
138 (0.7%)	309 (2%)	7.02 (10%) / N = 0.85	6.06 (4.4%) / N=0.44

Table S2. Summary of fitted data for bare FTO sample using a Randles modified cell^[2] equivalent circuit model in Figure 1b of the main manuscript. CPE is used instead of ideal capacitance (Q_{dl}) and Warburg element (Q_w) for increasing the quality of the fitting ($\chi^2 = 0.023$)

$$d = \frac{\varepsilon_0 \varepsilon_i A}{C} \quad (\text{Eq. S1})$$

where d is the thickness of the coating, C_c is the coating capacitance calculated using fitted values in Table S1, ε_0 is the permittivity of free space, ε_i is the dielectric constant of the coating ($3.9 < \varepsilon_i < 4.5$ as explained in the main manuscript), A the area of the electrode.^[3]

$$\Gamma = 1 - \frac{R_{ct}^{FTO}}{R_{ct}^{SAM}} \quad (\text{Eq. S2})$$

Where Γ is the percentage surface coverage, R_{ct}^i are the charge transfer resistance fitted values tabulated in Table S1 and Table S2.

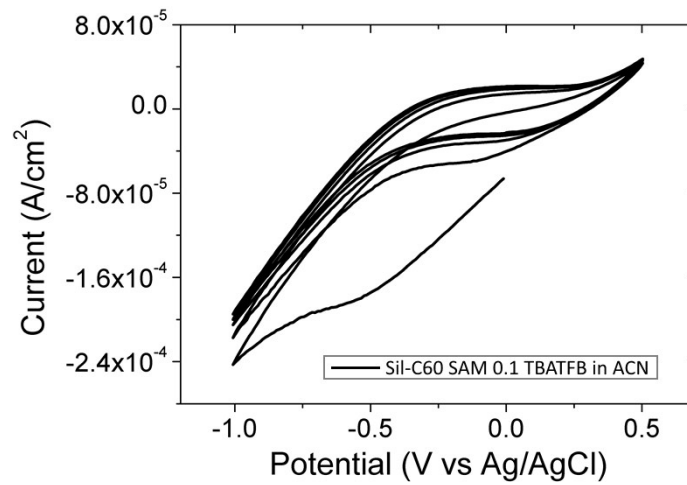


Figure S1. Stability test of a Sil-C60 SAM sample. Scan rate: 0.1 V/s

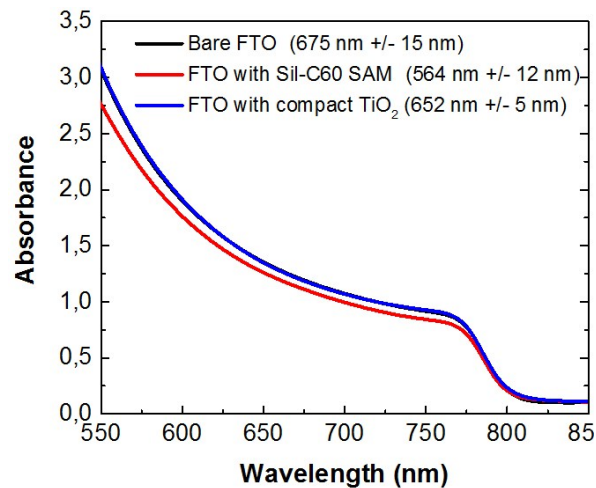


Figure S2. Optical absorption of perovskite films obtained on various substrates. The legend contains film thickness values measured by a profilometer.

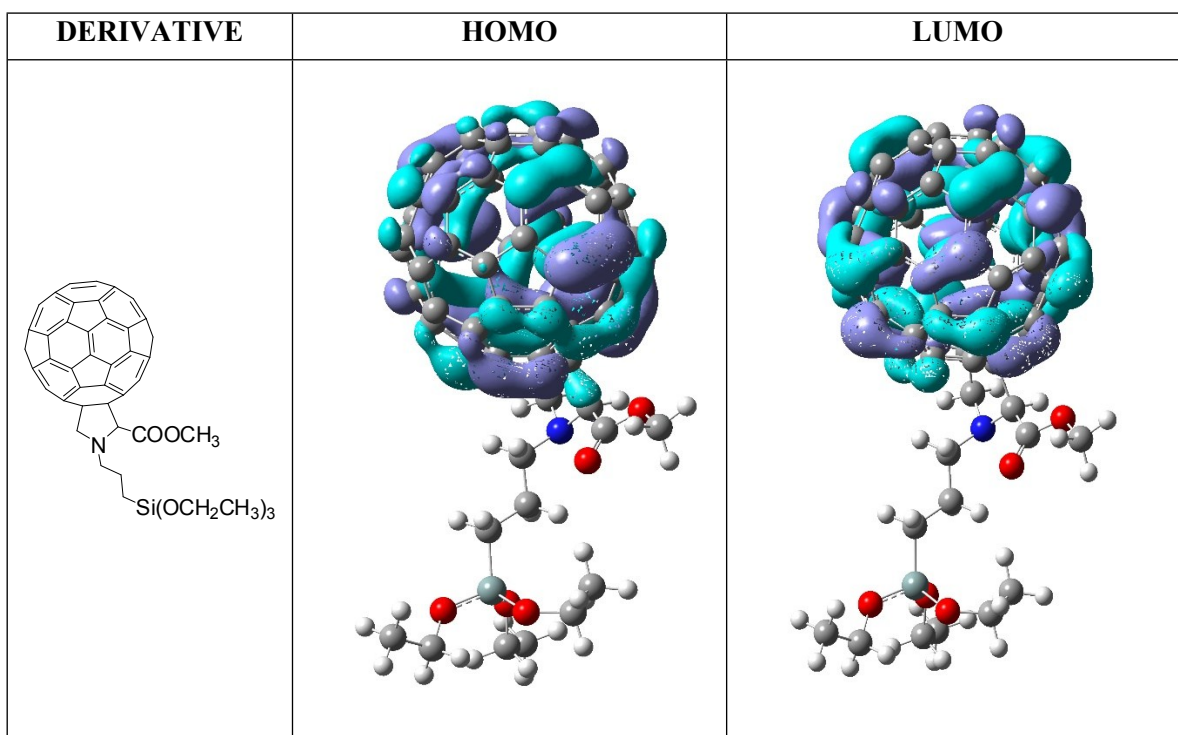


Figure S3. Isodensity surface plots of the HOMO-LUMO orbitals of Sil-C60.

Table S3. Computed HOMO-LUMO energies and band gaps for Sil-C60 and PCBM calculated B3LYP 6-311G**.

derivative	HOMO energy (eV)	LUMO energy (eV)	band-gap
Sil-C60	-6.04	-3.51	2.53
PCBM	-6.07	-3.52	2.55

a) O₂ plasma treated FTO, $2^\circ \pm 0.2^\circ$



b) cTiO₂, $21^\circ \pm 2^\circ$

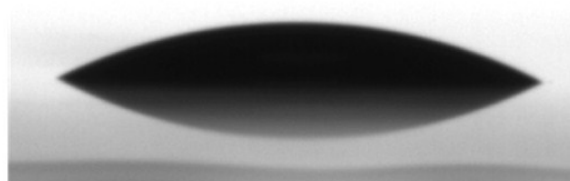


Figure S4. Wettability measurements of a) plasma treated FTO and b) compact TiO₂.

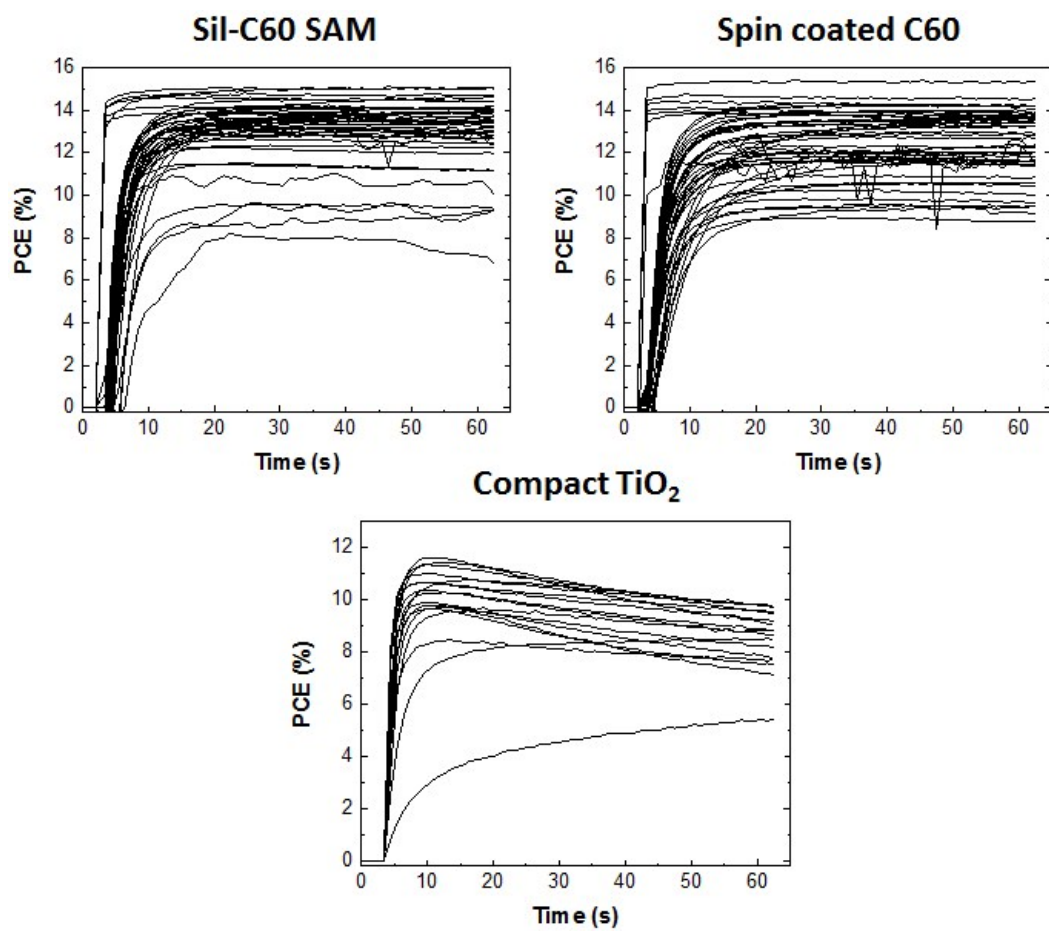


Figure S5. Time dependent PCEs obtained with solar cells employing Sil-C60 SAM, spin coated C60 and compact TiO₂ as ETL.

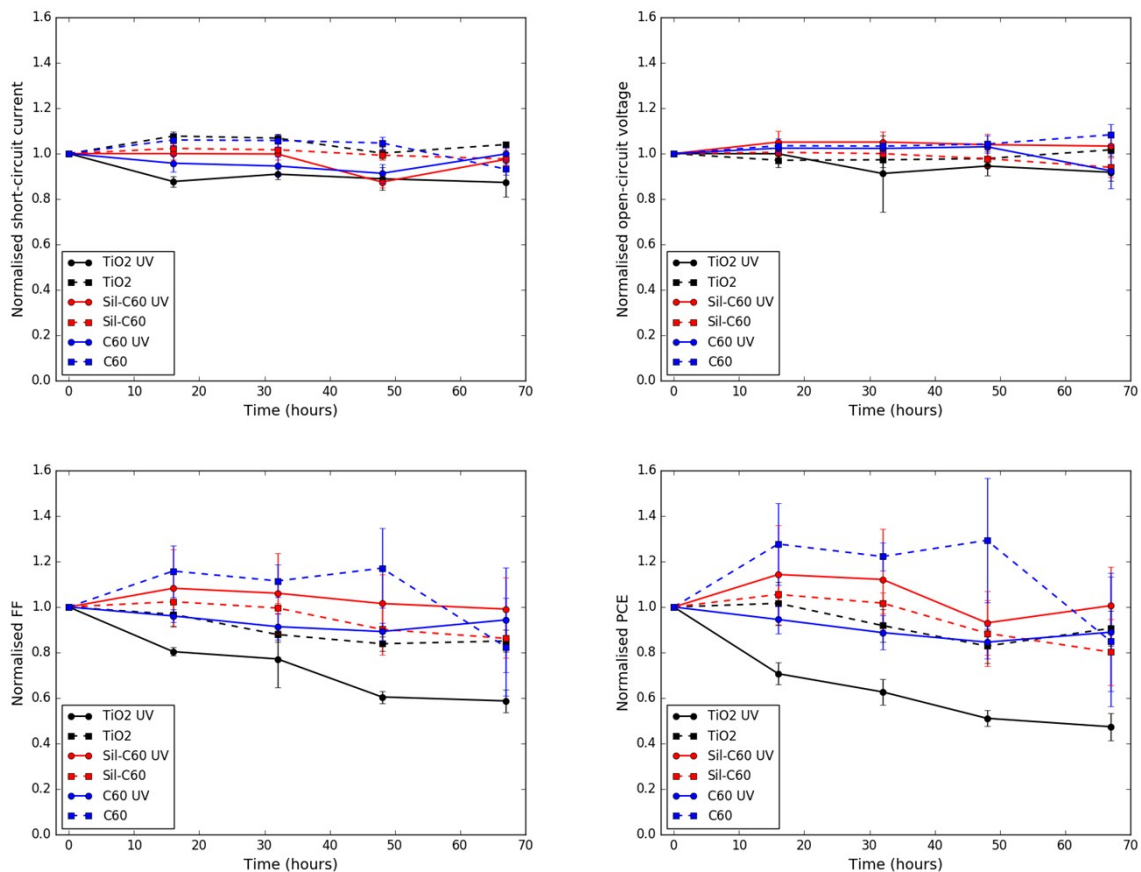


Figure S6. Degradation of solar cell parameters (higher efficiency scan direction, scanning from open-circuit to short-circuit) for cells stored under inert conditions with different electron-transport layers, with and without UV exposure, as indicated in the legend. Each parameter of each pixel is normalized to its as-prepared initial value. Data points are mean values and error bars are standard deviation from 6-8 pixels for each type of device.

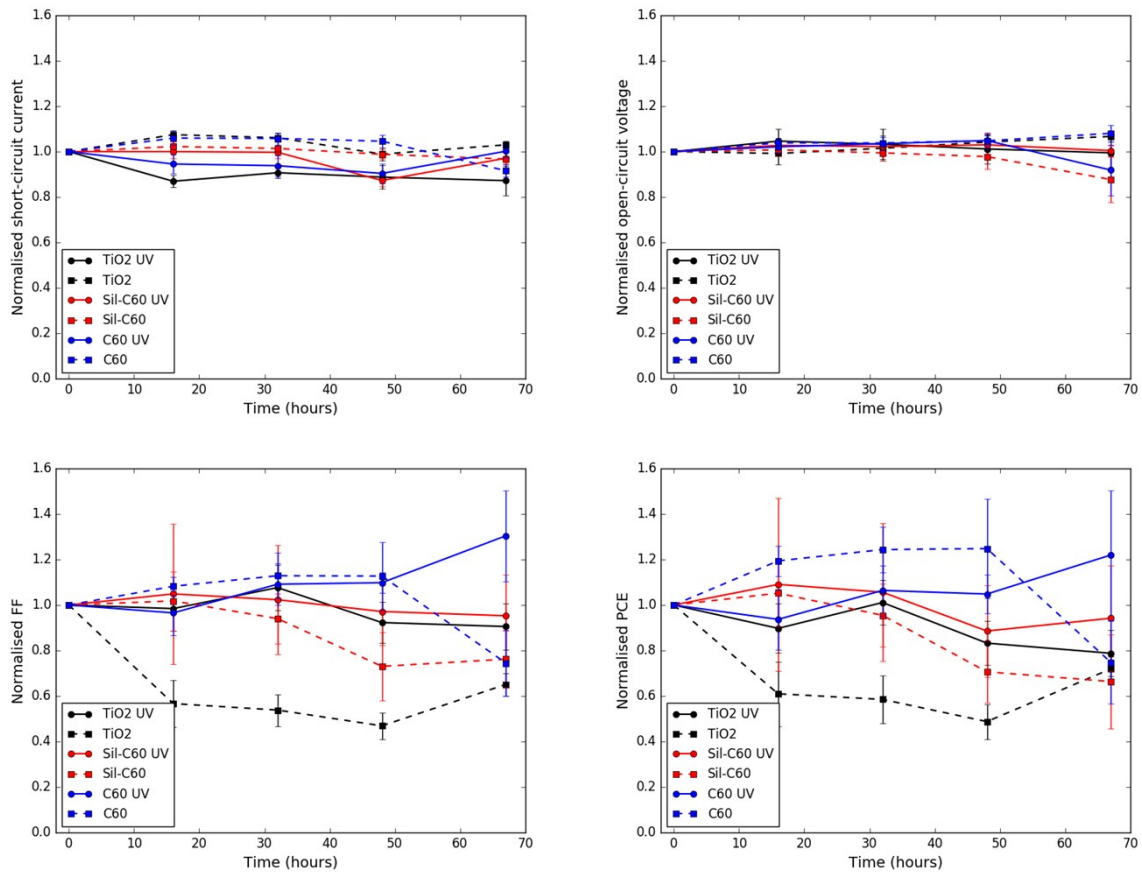


Figure S7. Degradation of solar cell parameters (lower efficiency scan direction, scanning from short-circuit to open-circuit) for cells stored under inert conditions with different electron-transport layers, with and without UV exposure, as indicated in the legend. Each parameter of each pixel is normalized to its as-prepared initial value. Data points are mean values and error bars are standard deviation from 6-8 pixels for each type of device.

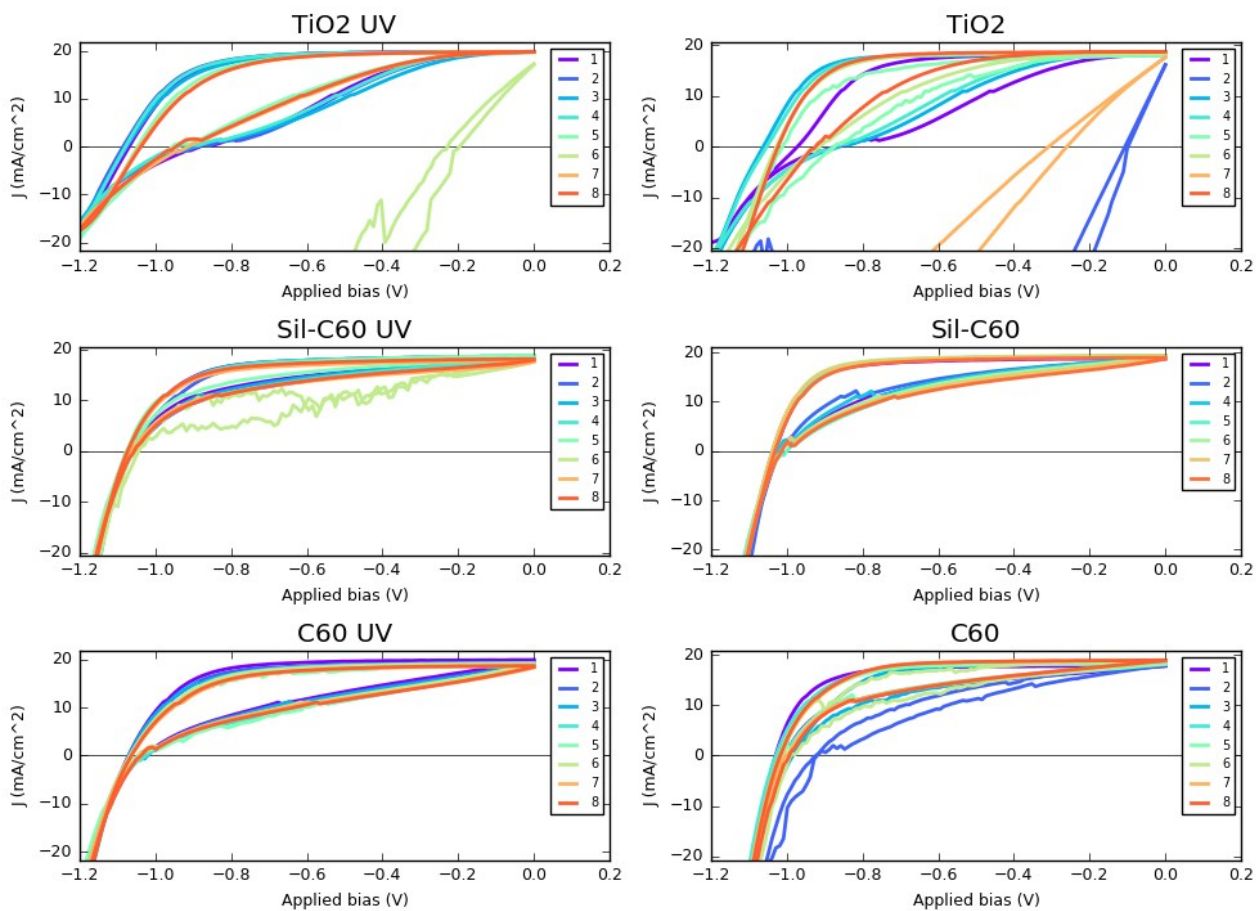


Figure S8. Current density-voltage characteristics for all pixels (pixel numbers indicated in the legend) of each cell type for freshly prepared devices.

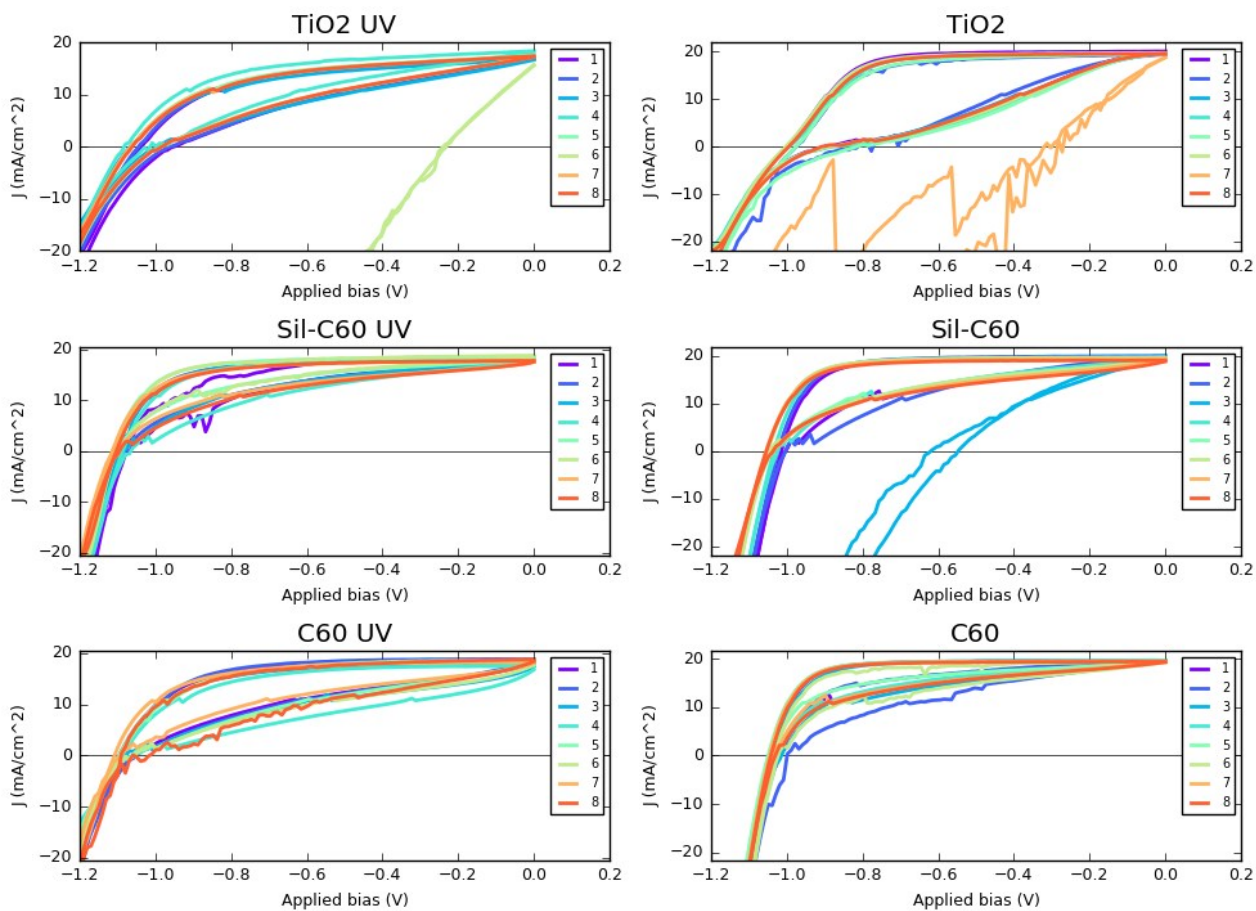


Figure S9. Current density-voltage characteristics for all pixels (pixel number given in the legend) of each cell type for devices stored under inert conditions for 16 hours, with or without UV light exposure.

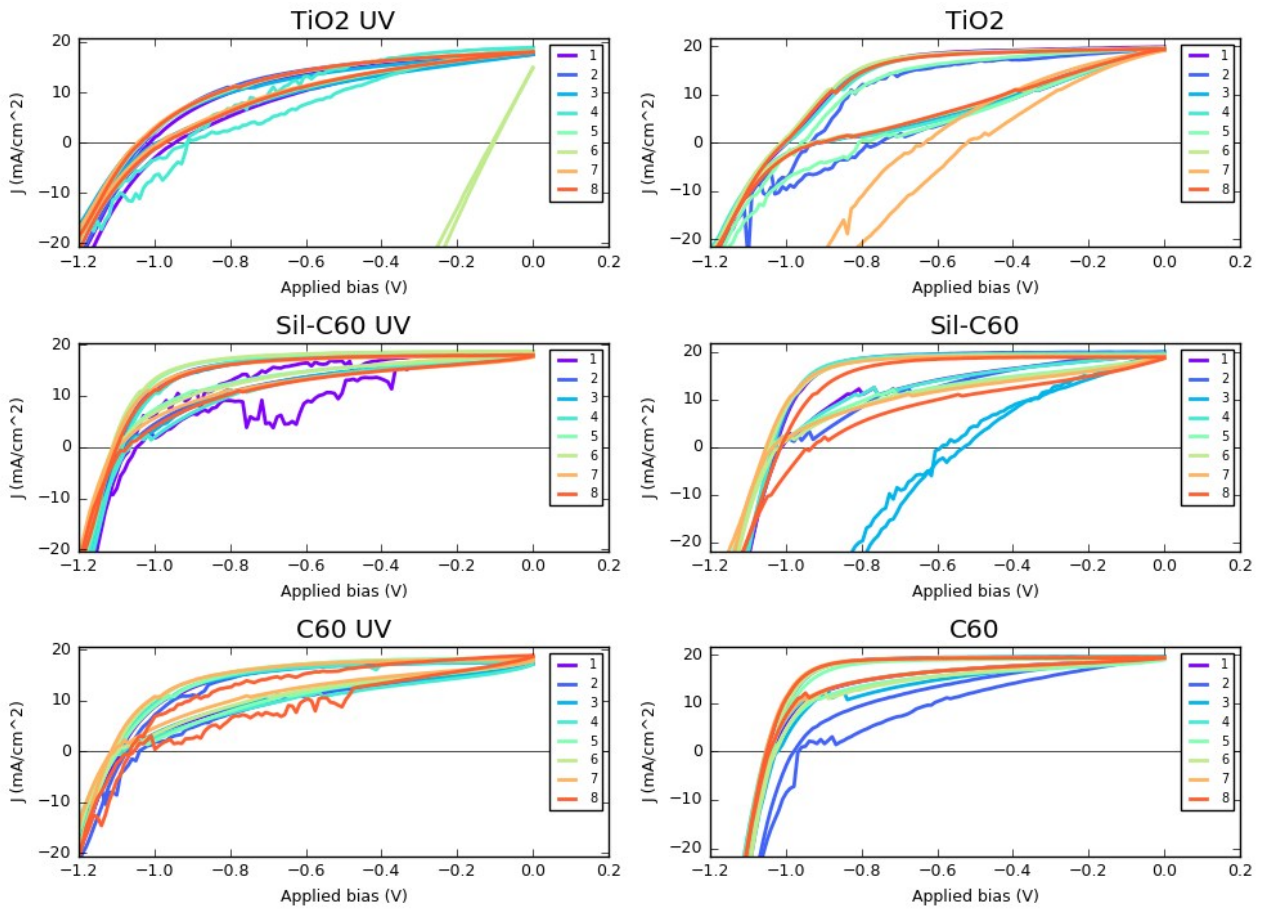


Figure S10. Current density-voltage characteristics for all pixels (pixel number given in the legend) of each cell type for devices stored under inert conditions for 32 hours, with or without UV light exposure.

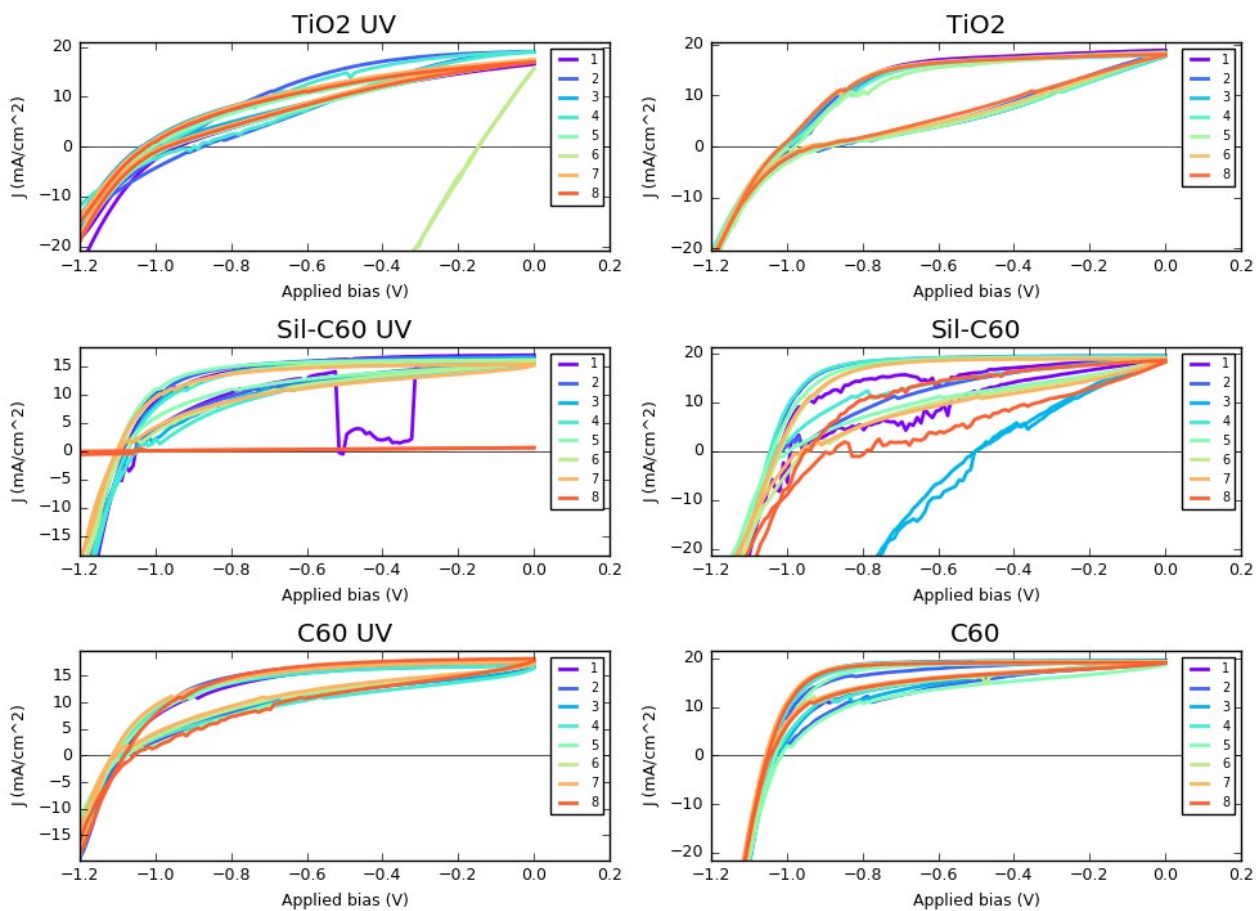


Figure S11. Current density-voltage characteristics for all pixels (pixel number given in the legend) of each cell type for devices stored under inert conditions for 48 hours, with or without UV light exposure.

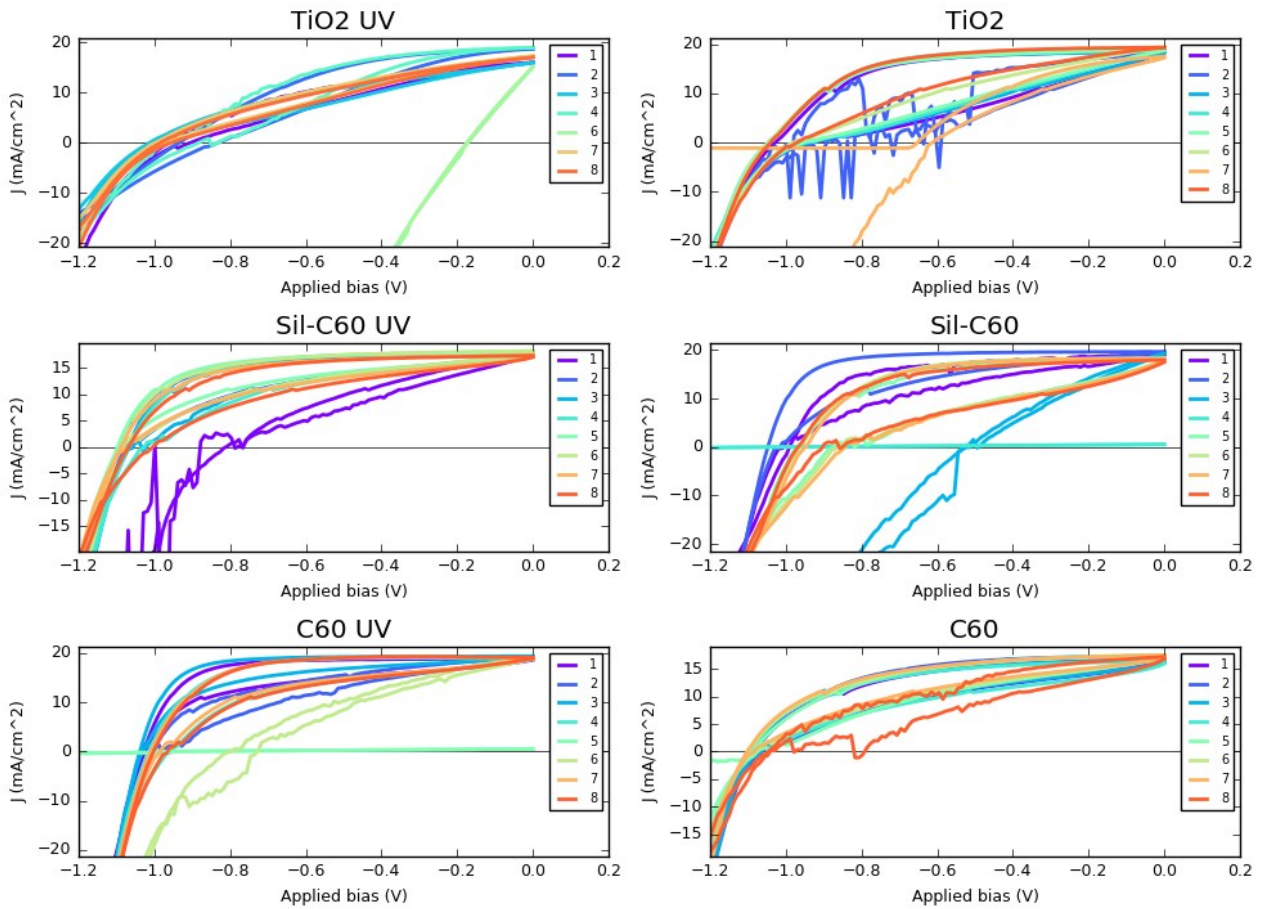


Figure S12. Current density-voltage characteristics for all pixels (pixel number given in the legend) of each cell type for devices stored under inert conditions for 60 hours, with or without UV light exposure.

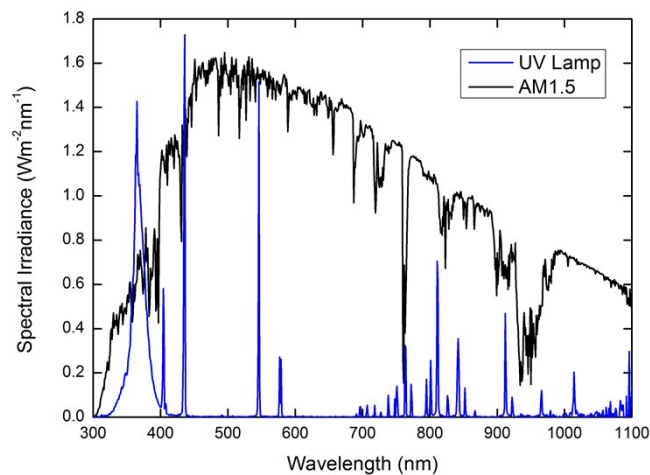


Figure S13. Spectral irradiance of the UV lamp used for UV stability testing alongside the AM1.5 solar spectrum.

References

- [1] A. Bianco, T. Da Ros, M. Prato, C. Toniolo, *J. Peptide Sci.* **2001**, 7, 208.

- [2] F. Lamberti, D. Ferraro, M. Giomo, N. Elvassore, *Electrochim. Acta* **2013**, 97, 304.
- [3] M. E. Orazem, B. Tribollet, *Electrochemical Impedance Spectroscopy*, John Wiley & Sons, **2011**.